Jawed vertebrates have three pairs of *Dlx* homeobox genes—*Dlx1/2*, *Dlx5/6*, and *Dlx3/7*—that are expressed in restricted domains across the proximodistal axis of the branchial arches (*4*). Their nested expression within the branchial arches and the fact that their *Drosophila* homolog *distalless* is a master regulator of distal leg identity make the *Dlx* genes excellent candidates for encoding distal identity in vertebrates. In all bilateral organisms, *distalless* genes appear to be involved in controlling the outgrowth of body appendages (*5*). Thus, the idea that the vertebrate *Dlx* homologs serve a similar function is attractive. Rather disappointingly, mice missing a single *Dlx* gene exhibit only piecemeal changes in the identities of isolated skeletal elements and teeth. This finding suggested that *Dlx* genes act as "micromanagers" rather than as "master regulators." Now, Depew and colleagues report the striking phenotype of the *Dlx5/6* double mutant mouse (*1*). They provide evidence that *Dlx5* and *Dlx6* are indeed the selectors of distal branchial arch identity. Their work suggests that the absence of a clear phenotype in mice lacking one *Dlx* gene is due to compensation by other coexpressed *Dlx* genes. Thanks to their discovery, the concept of a proximodistal molecular identity code is alive and well.

The phenotype of the *Dlx5/6* double mutant mouse is complex but remarkably clearcut. All of the skeletal elements below the primary jaw joint (the joint between the malleus and incus of the mammalian middle ear) are missing. Even more intriguing, in the region of the lower jaw, the mutant mice possessed a second complete set of bona fide upper jaw elements. During the early evolution of mammals, the major upper jaw element (the so-called palatoquadrate) became fragmented. Parts of the palatoquadrate became fused to the braincase—the "tennis racket"-shaped alisphenoid bone in figure 3E and supplementary figure 3D of the Depew *et al.* paper—or gave rise to elements of the mammalian pharynx (pterygoid). Other parts such as the quadrate turned into the mammalian incus, and the hyomandibula became the third middle ear bone (the stapes)—all elements of a new hearing apparatus (*6*). In the *Dlx5/6* double mutant mice all of these elements are duplicated, resulting in a symmetrical instead of an asymmetrical mouth.

If *Dlx5* and *Dlx6* are distal selector genes, then where does the initial patterning information for the branchial arch proximodistal axis come from? A recent elegant paper by Couly *et al.* sheds light on this difficult question (*7*). By transplanting pharyngeal endoderm into different locations in the developing chick head, Couly *et al.* generated jaw duplications that are remarkably similar to those obtained by Depew *et al.* (*1*). A growing body of evidence suggests that initial cues from the pharyngeal endoderm impose a first proximodistal patterning axis onto the adjacent branchial arch neural crest cells. This prepattern is then "interpreted" by neural crest cells, resulting in the nested expression of *Dlx* gene pairs, *Dlx5/6* and *Dlx3/7*, by these cells. If this is the case, what does the *Dlx5/6* mutant phenotype tell us about the evolution of jaws?

Although upper and lower jaw elements have never been completely symmetrical during vertebrate history, early jawed vertebrates related to the ancestors of bony fish (such as acanthodians) experimented with the shape and symmetry of their jaws. Acanthodians, for example, sometimes displayed remarkable symmetry between their upper and lower jaw elements (see the figure, part A, green) as well as in their dentition (see the figure, part B, yellow) (*8*). Such symmetrical features, which disappeared later in evolutionary history, now reappear in the *Dlx5/Dlx6* double mutant mice.

The Depew *et al.* work suggests that lower jaw patterning that is dependent on *Dlx5/6* expression may have been elaborated and embellished between the phylogenetic nodes of jawed vertebrate and bony fish ancestors. Going back one step further in evolutionary history, jawless vertebrates such as lampreys only have four *Dlx* genes with unclear homologies to their jawed vertebrate counterparts (*9*). All lamprey *Dlx* genes are expressed in branchial arches, but a nested expression pattern appears to be the invention of the jawed vertebrates (*10*). Our knowledge of the enhancer organization that controls this nested *Dlx* gene expression in jawed vertebrates is still rudimentary. Comparative genomic and functional studies of the regulatory elements controlling *Dlx* gene expression in lampreys, sharks, bony fish, coelacanths, and tetrapods will reveal the molecular evolution of the proximodistal code that underlies the shapes and fates of jaws.

References

1. M. J. Depew, T. Lufkin, J. R. Rubenstein, *Science* **298**, 381 (2002); published online 22 August 2002 (10.1126/science.1075703).
2. N. LeDouarin, C. Kalcheim, *The Neural Crest* (Cambridge Univ. Press, Cambridge, 1999).
3. G. Koentges, A. Lumsden, *Development* **122**, 3229 (1996).
4. M. Qiu *et al.*, *Dev. Biol.* **185**, 165 (1997).
5. G. Panganiban *et al.*, *Proc. Natl. Acad. Sci. U.S.A.* **94**, 5162 (1997).
6. E. Gaupp, *Arch. Anat. Entwickl. Gesch.* (suppl.), 1 (1912).
7. G. Couly *et al.*, *Development* **129**, 1061 (2002).
8. P. Janvier, *Early Vertebrates* (Clarendon, Oxford, 1996).
9. A. Neidert *et al.*, *Proc. Natl. Acad. Sci. U.S.A.* **98**, 1665 (2001).
10. Y. Shigetani *et al.*, *Science* **296**, 1316 (2002).

PERSPECTIVES: OPTICS

A New Low for Nonlinear Optics

M. C. Downer

In the first nonlinear optics experiment, Franken *et al.* (*1*) focused a 3-joule red ruby laser pulse into a quartz crystal to generate a few nanojoules of ultraviolet light at exactly twice the incident frequency. The photographic recording of the signal was so weak that the editor mistook it for a blemish and erased it before publication. The memory of nonlinear optics might have been erased, too, except that since then, a series of breakthroughs has increased the efficiency of many nonlinear optical frequency conversion processes by orders of magnitude, transforming them into useful tools for science and technology.

In the 1960s, researchers discovered a class of crystals, now standard in laser laboratories, that could convert pulses one-thousandth as strong as Franken's ruby pulse to another color with as much as 50% efficiency, simply by matching the index of refraction of the input and output frequencies (*2*).

In the 1990s, a new class of synthetic nonlinear optical multilayer structures was developed and commercialized that efficiently converted still weaker, fixed-frequency beams from small solid-state lasers to tunable visible and infrared radiation for applications in materials processing, remote sensing of environmentally sensitive gases, and interferometry (*3*).

Along an independent line, chemists discovered in the 1970s that another notoriously weak nonlinear optical process, spontaneous Raman scattering, used to fingerprint molecular vibrations (*4*), could be enhanced dramatically by attaching molecules to rough metal surfaces or metal nanoparticles (*5*). With this approach, Raman spectra of single molecules can now be measured (*6*).

On page 399 of this issue, Benabid *et al.* (*7*) report a breakthrough in the nonlinear optics of molecular gases that adds a new milestone to these historical examples. After pressurizing the hollow core (HC) of a meter-long glass photonic-crystal fiber (PCF) with hydrogen gas, the authors

The author is in the Physics Department, University of Texas, Austin, TX 78712, USA. E-mail: downer@physics.utexas.edu

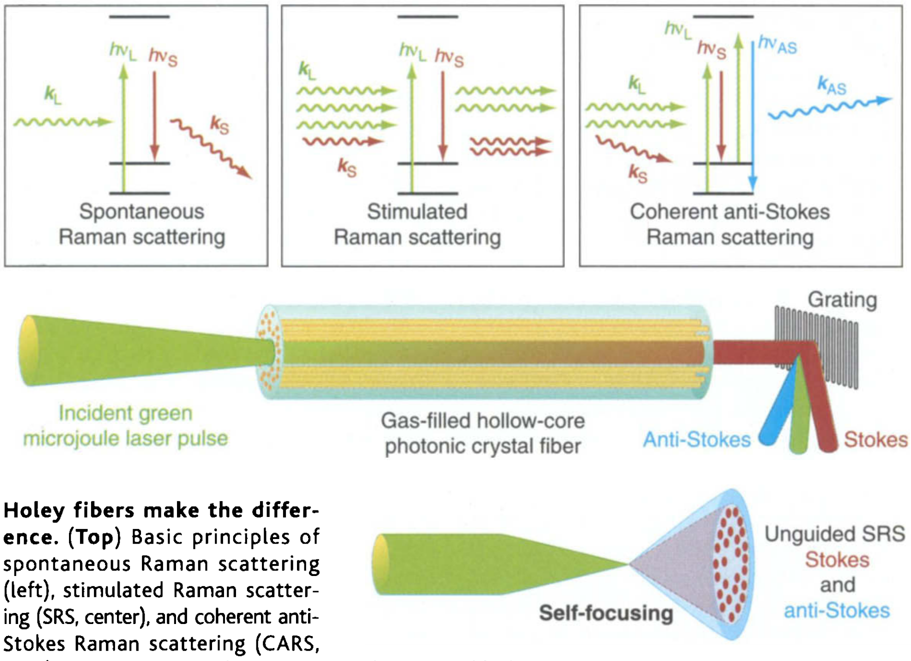

Holey fibers make the difference. (Top) Basic principles of spontaneous Raman scattering (left), stimulated Raman scattering (SRS, center), and coherent anti-Stokes Raman scattering (CARS, right). Straight arrows, photon energies; horizontal black lines, molecular energy levels; wavy lines, incident (left) and output (right) photon momenta. **(Middle)** SRS and CARS in a holey fiber are characterized by unusually low input energy and high mode quality of the generated beams. **(Bottom)** Poor beam quality is typical of unguided SRS because of uncontrolled self-focusing and the phase-matching requirements of the CARS process.

demonstrate that green laser pulses propagating through the core with microjoule energy—two orders of magnitude weaker than previous demonstrations in gases—convert efficiently (30%) to red pulses by stimulated Raman scattering (SRS) (*8*) from the hydrogen stretch vibration (see the figure, middle panel). Reductions in fiber loss and laser line width, and an increase in fiber length, should lower the threshold energy for gas-phase SRS even further.

In spontaneous Raman scattering, an incident photon ($h\nu_L$) scatters inelastically from the sample, emerging as a lower energy "Stokes" photon ($h\nu_S$), depositing the energy difference $h\Delta\nu = h(\nu_L - \nu_S)$ into an electronic, vibrational, or rotational excitation (see the figure, top left) (*4*–*6*). In SRS, a "seed" of Stokes (ν_S) light, usually from prior spontaneous Raman scattering, impinges on the sample simultaneously with "pump" (ν_L) light, and grows exponentially into a coherent, Stokes-shifted laser beam with gain proportional to the pump power and the spontaneous Raman cross section (see the figure, top center). The growing Stokes wave can interact back with the pump to create an accompanying anti-Stokes wave ($\nu_L + \Delta\nu$) through the nonlinear process of coherent anti-Stokes Raman scattering (CARS) (see the figure, top right) (*8*).

The two closely linked processes of SRS and CARS have spawned a useful family of Raman-shifted lasers that provides coherent radiation at frequencies inaccessible from the source laser (*8*). However, such applications usually require powerful pump pulses and dense Raman media (solids, liquids, and high-pressure molecular gases) to achieve useful gain levels. SRS is then easily disrupted by another nonlinear process, self-focusing, which degrades the mode quality and hence the usefulness of the generated beams (see the figure, bottom) (*8*).

The novel waveguide developed by Benabid *et al.* maintains small, smooth, well-overlapped pump and Stokes mode profiles, so that the Stokes wave grows in a controlled manner. Moreover, because pump and Stokes waves are automatically phase-matched in SRS, high conversion is possible with very low input powers and Raman cross sections, for long, low-loss fibers. Reduction of the linear loss of the HC-PCF to levels typical of traditional glass fibers should therefore allow the SRS gain threshold to be reduced further.

Traditional glass-core single-mode fibers have been used for some time to control and enhance SRS and other nonlinear optical interactions of weak light pulses (*9*). SRS from the Si-O bonds of the silica core, pumped by semiconductor lasers, is emerging as a crucial amplification technology for modern high-speed, long-distance fiber optic transmission systems (*10*). These fibers guide light by total internal reflection, made possible by the high refractive index of the glass core.

To enhance nonlinear optics in gases, some previous researchers have used gas-filled capillary guides (*11*, *12*). But total internal reflection is lost because gases have refractive indices close to 1, whereas all capillary wall materials have larger refractive indices. Thus, all modes leak, and relatively large cores are required to avoid diffraction losses. Large cores mean large energy and multiple transverse modes—and hence poor beam quality.

Three years ago, some of the authors of the current study reported single-mode guidance of low-intensity light in a 3-cm-long HC-PCF. Instead of total internal reflection, Bragg diffraction from an ordered array of cladding resonators surrounding the core guided the light (*13*). However, neither SRS nor any nonlinear frequency conversion process would have been possible in that fiber, because single-mode guiding was limited to a few narrow-wavelength windows—the photonic band gaps.

For the present work, the authors developed a new, longer HC-PCF with a transmission bandwidth covering the whole visible and infrared range. Consequently, both the incident and frequency-converted pulses propagate through the gas with single, high-quality transverse mode profiles.

Relative to their solid-state counterparts, gaseous nonlinear media are cheap, replenishable, interchangeable, and variable in density, and they exhibit sharp spectral lines. Thus, gas-filled holey fibers are likely to provide versatile Raman shifters for low-power, narrow-bandwidth solid-state lasers. In addition, they should enable high-resolution SRS spectroscopy (*14*) of trace gases with unprecedented sensitivity for remote sensing applications, because SRS—unlike its spontaneous counterpart—is not limited by spectrometer resolution and yields a coherent directional Stokes signal.

Additional possibilities will open up if researchers find a way to propagate more powerful pulses through gas-filled HC-PCFs. Benabid *et al.* see evidence that self-focusing, the bane of traditional SRS, disrupts the mode and induces loss at peak powers above a kilowatt. This threshold should rise in less dense gases. It may then be possible to generate a cascade of mutually coherent higher order Stokes and anti-Stokes frequencies, and phase-lock them to create femtosecond pulses out of pulsed or continuous input beams (*15*). Propagation of femtosecond pulses near the gas ionization threshold in holey fibers may enable generation of soft x-ray beams with better efficiency and beam quality than previously demonstrated (*12*). Wide continuous tuning of such pulses by ionization-induced blueshifting may become possible (*16*).

Perhaps pulses with intensity well above the gas ionization threshold might even propagate through the gas-filled core. We can base this hope on the success of Dorchies *et al.* in propagating pulses more than a thousand times the ionization threshold ($\sim 10^{16}$

W/cm^2) through a conventional gas-filled hollow capillary without damaging the walls (*17*). This possibility would open new directions in laser-plasma nonlinear optics, including laser-plasma acceleration of charged particles and laser-plasma Raman amplifiers that can withstand unprecedented intensities (*18*).

Benabid *et al.* report the first step toward these exciting possibilities for nonlinear optics with hollow-core fibers. A new era in the nonlinear optics of gases, and maybe even plasmas, is about to begin.

References and Notes

1. P. Franken, A. E. Hill, C. W. Peters, G. Weinrich, *Phys. Rev. Lett.* **7**, 118 (1962).
2. V. G. Dmitriev, G. G. Gurzadyan, D. N. Nikogosyan, *Handbook of Nonlinear Optical Crystals* (Springer-Verlag, New York, ed. 3, 1999).
3. M. Fejer, *IEEE J. Quantum Electron.* **28**, 2631 (1992).
4. C. V. Raman, K. S. Krishnan, *Indian J. Phys.* **2**, 399 (1928).
5. A. Otto, in *Light Scattering in Solids IV*, M. Cardona, G. Guntherodt, Eds. (Springer, Berlin, 1984), p. 289.
6. S. Nie, S. R. Emory, *Science* **275**, 1102 (1997).
7. F. Benabid *et al.*, *Science* **298**, 399 (2002).
8. N. Bloembergen, *Am. J. Phys.* **35**, 989 (1967).
9. G. P. Agrawal, *Nonlinear Fiber Optics* (Academic Press, San Diego, CA, ed. 2, 1989).
10. V. E. Perlin, H. G. Winful, *J. Lightwave Technol.* **20**, 409 (2002).
11. G. Korn, O. Dühr, A. Nazarkin, *Phys. Rev. Lett.* **81**, 1215 (1998).
12. A. R. Rundquist *et al.*, *Science* **280**, 1412 (1998).
13. R. F. Cregan *et al.*, *Science* **285**, 1537 (1999).
14. A. Owyoung, in H. Walther, K. W. Rothe, Eds., *Laser Spectroscopy IV* (Springer, Berlin, 1979), p. 175.
15. A. V. Sokolov, D. D. Yavuz, S. E. Harris, *Opt. Lett.* **24**, 557 (1999).
16. W. M. Wood, C. W. Siders, M. C. Downer, *Phys. Rev. Lett.* **67**, 3523 (1991).
17. F. Dorchies *et al.*, *Phys. Rev. Lett.* **82**, 4655 (1999).
18. G. Shvets, N. J. Fisch, A. Pukhov, J. Meyer-ter-Vehn, *Phys. Rev. E* **60**, 2218 (1999).

19. Supported by NSF and the Robert Welch Foundation.

PERSPECTIVES: BIOMINERALIZATION

At the Cutting Edge

Steve Weiner and Lia Addadi

In 1962, Heinz Lowenstam discovered that the outer layer of the teeth of a common intertidal mollusk, the chiton, is composed of magnetite (*1*) (see the figure, top panel). This magnetic iron oxide mineral was then thought to form only at elevated temperatures and pressures. The discovery focused attention on the ability of living systems to produce unexpected minerals, and proved to be a turning point for the field then known as calcification.

Forty years on, Lichtenegger *et al.* (*2*) report more dental surprises. On page 389 of this issue, they show that a copper chloride mineral, atacamite, is formed in the teeth of the carnivorous marine worm *Glycera* (see the figure, left panel). It is the first copper mineral to be identified that is formed under controlled conditions in an organism (*3*), prompting the question of how they can scavenge enough copper from their surroundings to produce this mineral.

The mineral atacamite is the latest addition to the growing list of known biological minerals. This list, compiled and monitored periodically by Lowenstam for more than 30 years, has expanded from just over 10 in the early 1960s to almost 70 today (see table S1 for a full listing). Many of the minerals do not contain calcium, prompting a change in the name of the field to biomineralization.

Atacamite reinforces the very sharp tips of four teeth that are used by the worms as syringes to inject poisonous venom into their prey. There is no definitive explanation for why they use copper. Another, taxonomically related, worm (*4*), and quite a few arthropods, have high concentrations of zinc in their teeth

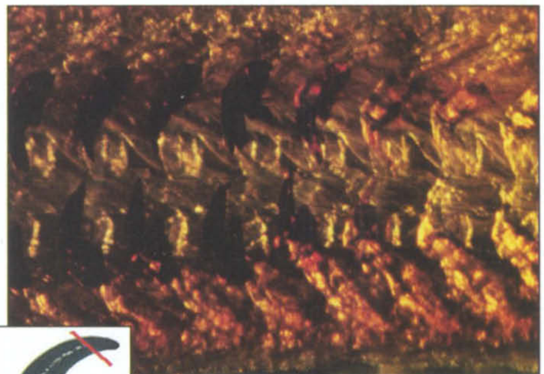

Dental treatment. (Top) The radula of the giant cryptochiton is analogous to an assembly line, with tooth formation progressing from right to left. The translucent teeth on the right are composed only of an organic matrix framework. The red-colored teeth in the center contain ferrihydrite, an iron oxide precursor of magnetite. The latter is present in the black-colored teeth on the left [reviewed in (*9*)]. The chiton radula represents one of the best-documented examples of a preformed organic framework in which mineral subsequently forms. This basic strategy is widespread in biomineralization. It also demonstrates that transient mineral phases may be the first deposits during mineralization. **(Left)** The teeth of the bloodworm *Glycera*, shown by Lichtenegger *et al.* (*2*) to contain a copper mineral.

CREDIT: TOP PANEL, H. A. LOWENSTAM; LEFT PANEL FROM (2)

and mandibles (*5*). The zinc is apparently not in the form of a mineral, but is associated directly with the organic framework. One intriguing possibility raised by the authors is that the copper may activate the venom as it is being injected. Lichtenegger *et al.* also point out that atacamite [$Cu_2(OH)_3Cl$] occurs in four different polymorphic forms. As the worm consistently forms only one, the process must be under strict chemical control.

The field of biomineralization straddles the organic and inorganic worlds. The "active site" equivalent of a mineralized tissue is the interface at which the biological macromolecules that control mineral formation interact with the mineral surfaces. The major component of the teeth of the worms studied by Lichtenegger *et al.* (*2*) is an unusual and uncharacterized protein (or protein mixture) rich in glycine and histidine (*6*). Histidine is a common ligand in metal-binding sites of metalloenzymes, including those containing copper. It will be most interesting to understand the nature of the interface between this structural protein and atacamite.

Many fundamental questions remain to be addressed regarding recognition and assembly in complex three-dimensional biological tissues such as teeth. Understanding these processes in the vertebrate skeleton and in tooth formation, and in the many forms of human pathology involving mineral formation, has much relevance to medicine.

About a decade ago, materials scientists began to look for new ideas for improving materials design inspired by biological materials. Lichtenegger *et al.* (*2*) elegantly show that the teeth of their worms have an extraordinary resistance to abrasion. This property is presumably related to the molecular structure of the mineral-reinforced fibrils that constitute the building block of the tooth. Such mineralized fibrils are common in biological tissues, including vertebrate bone and tooth dentin (*7*). Understanding the structural basis for this unusual mechanical property in the worm teeth could lead to new ideas for tool design. Many other scientific disciplines including paleoclimatology, archaeology, evolution, and paleontology, which extensively use biologically produced skeletons, may also benefit.

With the discovery of biogenic atacamite formed by a group of exotic blood worms, another fascinating window on the field of biomineralization opens up. Understanding how copper is scavenged, transported, and concentrated, and ultimately how this particular mineral is induced to form with its own

The authors are in the Department of Structural Biology, Weizmann Institute of Science, Rehovot 76100, Israel. E-mail: steve.weiner@weizmann.ac.il, lia.addadi@weizmann.ac.il